

# Synthesis of an Undecasaccharide Featuring an Oligomannosidic Heptasaccharide and a Bacterial Kdo-lipid A Backbone for Eliciting Neutralizing Antibodies to Mammalian Oligomannose on the HIV-1 Envelope Spike

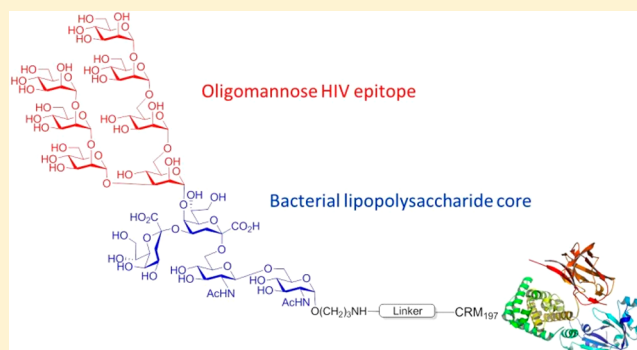
Nino Trattinig,<sup>†</sup> Markus Blaukopf,<sup>†</sup> Jean-François Bruxelles,<sup>‡</sup> Ralph Pantophlet,<sup>‡,§</sup> and Paul Kosma<sup>\*,†</sup> 

<sup>†</sup>Department of Chemistry, University of Natural Resources and Life Sciences, A-1190 Vienna, Austria

<sup>‡</sup>Faculty of Health Sciences and <sup>§</sup>Department of Molecular Biology and Biochemistry, Simon Fraser University, Burnaby, British Columbia V5A 1S6, Canada

## Supporting Information

**ABSTRACT:** Lipooligosaccharides (LOS) from the bacterium *Rhizobium radiobacter* Rv3 are structurally related to antigenic mammalian oligomannoses on the HIV-1 envelope glycoprotein spike that are targets for broadly neutralizing antibodies. Here, we prepared a hybrid structure of viral and bacterial epitopes as part of a vaccine design strategy to elicit oligomannose-specific HIV-neutralizing antibodies using glycoconjugates based on the Rv3 LOS structure. Starting from a Kdo<sub>2</sub>GlcNAc<sub>2</sub> tetrasaccharide precursor, a central orthogonally protected mannose trichloroacetimidate donor was coupled to OH-5 of the innermost Kdo residue. To assemble larger glycans, the *N*-acetyl amino groups of the glucosamine units were converted to imides to prevent formation of unwanted imidate byproducts. Blockwise coupling of the pentasaccharide acceptor with an  $\alpha$ -(1→2)-linked mannotriosyl trichloroacetimidate donor introduced the D1-arm fragment. Glycosylation of *O*-6 of the central branching mannose with an  $\alpha$ -(1→2)- $\alpha$ -(1→6)-linked mannotriosyl trichloroacetimidate donor unit then furnished the undecasaccharide harboring a D3-arm extension. Global deprotection yielded the 3-aminopropyl ligand, which was activated as an isothiocyanate or adipic acid succinimidoyl ester and conjugated to CRM<sub>197</sub>. However, representative oligomannose-specific HIV-neutralizing antibodies bound the undecasaccharide conjugates poorly. Possible reasons for this outcome are discussed herein along with paths for improvement.



## ■ INTRODUCTION

HIV-1 remains a major threat to human health in many countries, and it is generally agreed that only a prophylactic vaccine is likely to curb infection rates globally.<sup>1,2</sup> To be effective, an HIV vaccine may need to elicit both humoral and cellular immune responses to blunt infection and protect against disease. The sole target for protective anti-HIV antibodies is the virus envelope spike (Env),<sup>3</sup> a densely glycosylated trimer of heterodimeric gp120 and gp41 subunits. The glycans on Env derive from the biosynthetic machinery of the mammalian host cell and are meant to allow the virus to evade the host antibody response.<sup>4</sup> As such, it was long thought that these glycans are immunologically silent.<sup>5</sup> However, over the last several years, it has become evident that some HIV-infected individuals develop neutralizing antibodies to this “glycan shield”.<sup>6</sup> 2G12 was the first human monoclonal antibody described that targets the glycans on HIV Env.<sup>7</sup> Later studies showed that 2G12 binds an array of oligomannoses on Env.<sup>8</sup> Following an extended period without any description of 2G12-like antibodies, the past decade has

seen a sharp increase in the discovery of additional neutralizing antibodies, some with substantial breadth and potency, targeting what is now defined as the “high-mannose patch” on HIV gp120.<sup>9</sup> Consequently, the high-mannose patch has gained substantial attraction as a target for vaccine development.<sup>10</sup> The lipooligosaccharide (LOS) of the phytopathogenic *Rhizobium radiobacter* strain Rv3 was shown previously to consist of a mannotetraose subunit  $\alpha$ -Man-(1→2)- $\alpha$ -Man-(1→2)- $\alpha$ -Man-(1→3)- $\alpha$ -Man that resembles the so-called D1 arm of mammalian oligomannose (Figure 1).<sup>11</sup> The antigenic similarity to mammalian oligomannose was shown by binding to 2G12, which is specific for the D1 arm oligomannose, and later confirmed by the crystal structure of the bacterial mannotetraose fragment in complex with 2G12.<sup>12</sup> The crystal structure of the bacterial ligand was then used to model and construct derivatives that would more closely resemble

Received: March 15, 2019

Published: April 22, 2019

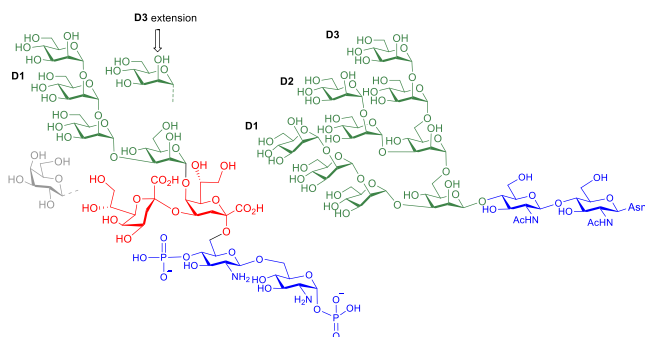


**Figure 1.** Structure of the LOS from *R. radiobacter* strain Rv3 (left) and of full-sized N-linked mammalian oligomannose (Man<sub>5</sub>GlcNAc<sub>2</sub>) (right). Dashed lines indicate substoichiometric substitution of the LOS by a mannosyl residue at O-6 of the central branching mannose and a galactosyl residue at O-8 of the side chain Kdo.

oligomannose, for example, by including a D3-arm surrogate to position 6 of the central mannose unit (Figure 1).<sup>13</sup>

A small library of two pentamannosides and four heptamannosides was synthesized previously as spacer-equipped ligands, which were then converted into their respective BSA conjugates.<sup>13</sup> BSA neoglycoconjugates containing the heptasaccharide  $\alpha$ -Man-(1 $\rightarrow$ 2)- $\alpha$ -Man-(1 $\rightarrow$ 2)- $\alpha$ -Man-(1 $\rightarrow$ 3)-[ $\alpha$ -Man-(1 $\rightarrow$ 2)- $\alpha$ -Man-(1 $\rightarrow$ 6)- $\alpha$ -Man-(1 $\rightarrow$ 6)]- $\beta$ -Man were bound best by the broadly neutralizing antibody PGT128 and related antibodies that target the oligomannose patch on Env.<sup>13</sup> Lesser binding of the antibodies to a related heptasaccharide conjugate containing the reducing mannose unit in the  $\alpha$ -anomeric configuration—as present in the bacterial glycan—suggested that the  $\beta$ -anomeric configuration better mimics the cognate epitope in this context. Nevertheless, it was possible to crystallize the soluble  $\alpha$ -anomeric heptamannoside ligand (dubbed NIT68A) in complex with PGT128, which showed that the interactions between antibody and the antigenic mimic versus mammalian oligomannose are essentially superimposable.<sup>13</sup> Human-antibody transgenic animals immunized with the  $\beta$ -anomeric heptamannoside conjugate yielded antibodies with the capacity to neutralize a few HIV strains, albeit at generally modest titers.<sup>13</sup>

Based on encouraging results from the series of studies summarized above, we have now set out to construct neoglycoconjugates that incorporate a distinctive bacterial constituent. Our goal is to obtain derivatives that more closely resemble bacterial LOS, thus increasing the “foreignness” of the glycosides and, presumably, their immunogenic potential. Our strategy is based on mimicry of host glycans by bacterial glycans, which trigger relatively robust antibody responses to otherwise poorly immunogenic epitopes. For example, animals immunized with purified *Campylobacter jejuni* LOS produce sustained levels of anti-LPS antibodies with ganglioside cross-reactivity.<sup>14</sup> Similarly, animals immunized with *Helicobacter pylori* cells or purified *H. pylori* LPS produce robust antibodies with capacity to bind Lewis X or Y antigens on human cells and tissue.<sup>15</sup>

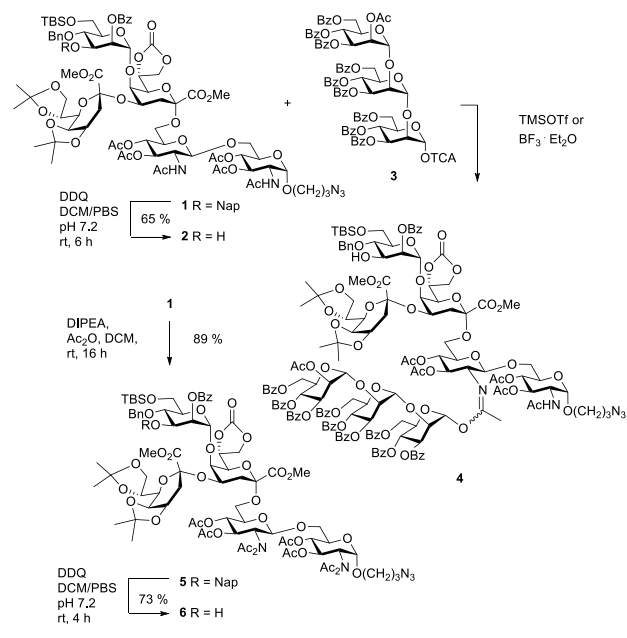
We recently communicated the chemical synthesis of the rhizobial pentasaccharide LOS core comprising the central  $\alpha$ -Man-(1 $\rightarrow$ 5)-linked Kdo<sub>2</sub>GlcNAc<sub>2</sub> unit.<sup>16</sup> The protected pentasaccharide had already been equipped with an orthogonal protecting group pattern at the central mannose which would allow the further extension at position 3 with the D1 arm and thus enable access to a defined material of the rhizobial

octasaccharide LOS. Moreover, selective removal of a 6-O-silyl ether had been foreseen which would open an access to incorporate the D3-arm surrogate chain. Here, we describe the chemical synthesis of this novel undecasaccharide, featuring a hybrid structure of viral and bacterial epitopes, its conversion into a CRM<sub>197</sub> neoglycoconjugate and binding studies with the HIV-broadly neutralizing antibody PGT128 and other select members of the PGT128/PGT130 neutralizing antibody family.

## RESULTS AND DISCUSSION

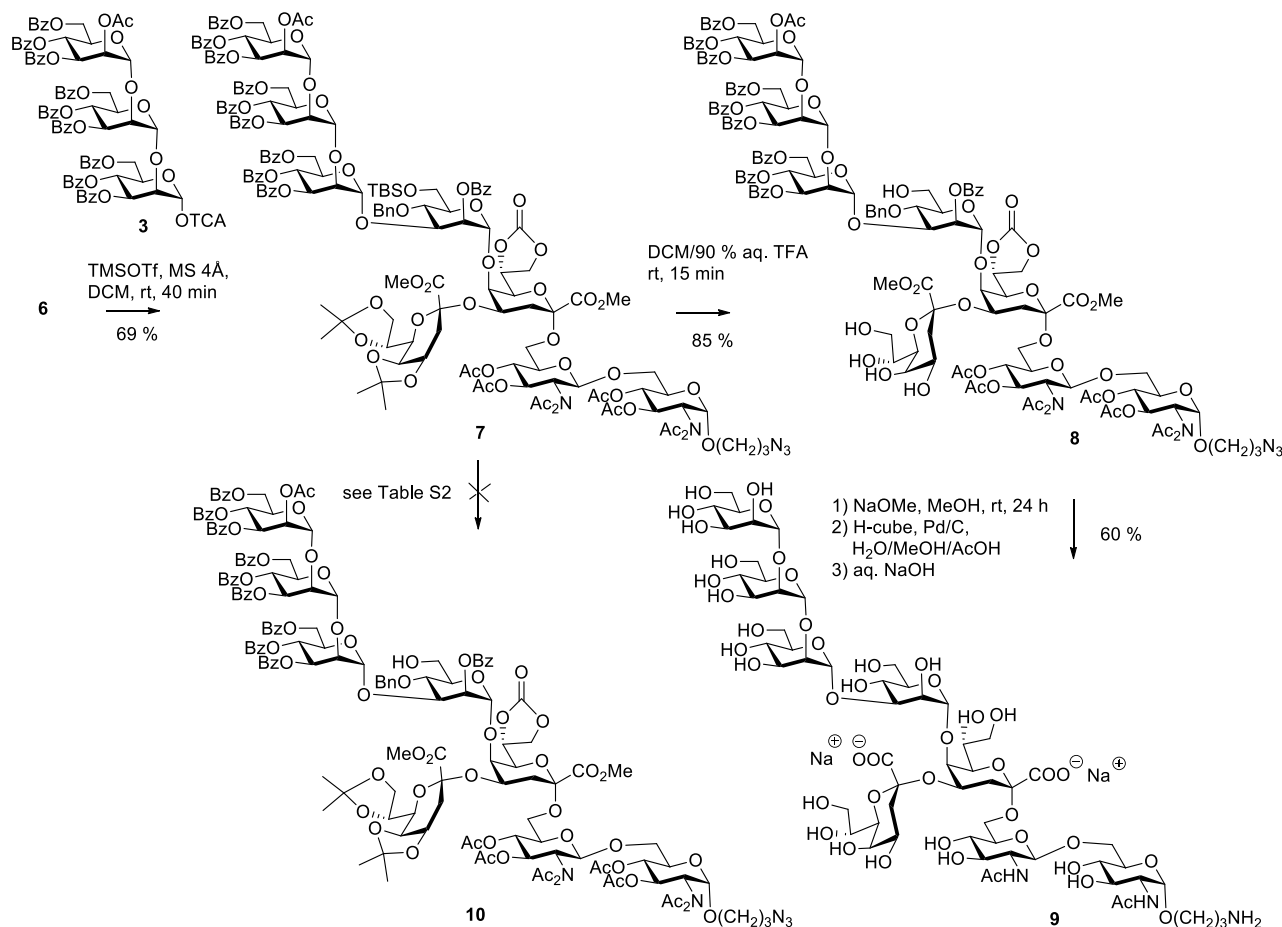
Aiming first at the rhizobial octasaccharide target, the previously reported pentasaccharide **1**, containing the  $\alpha$ -(1 $\rightarrow$ 5)-linked, orthogonally protected mannose unit, was subjected to DDQ oxidation to liberate position 3 for further extension (Scheme 1). Removal of the 3-O-(2-methylnaphthyl) group,

### Scheme 1. Imidate Formation and Synthesis of Pentasaccharide Acceptor **6**



however, could not be executed to full conversion, as degradation reactions started to occur leading to partial and complete loss of the isopropylidene groups at the lateral Kdo residue. By application of a mild basic buffer (PBS, pH = 7.2), hydrolysis was largely suppressed and compound **2** was eventually isolated in 65% yield by column chromatography with recovery of unreacted starting material (22%). The pronounced lability of the acetonide groups was also observed for solutions of **1** in CDCl<sub>3</sub> in an NMR tube upon standing for several hours. Hence, glycosyl acceptor **2** was directly used for the ensuing coupling reaction with the previously described<sup>13</sup> mannosyl trichloroacetimidate donor **3** in a [5 + 3] block assembly. Promotion of the glycosylation reaction either with TMSO triflate (0.15–2 equiv) or BF<sub>3</sub>·Et<sub>2</sub>O (2 equiv), respectively, resulted in formation of several byproducts and poor yields of glycoside. As the main reaction product, imidate-connected pseudo-octasaccharide **4** could be isolated in 37% yield from the reaction mixture together with unreacted acceptor **2** (23%). The structure of the imidate **4** was derived from proton and carbon NMR data, which revealed the loss of one NH signal of the GlcNAc-backbone and showed a

Scheme 2. Synthesis of Rhizobial LOS Octasaccharide Fragment 9



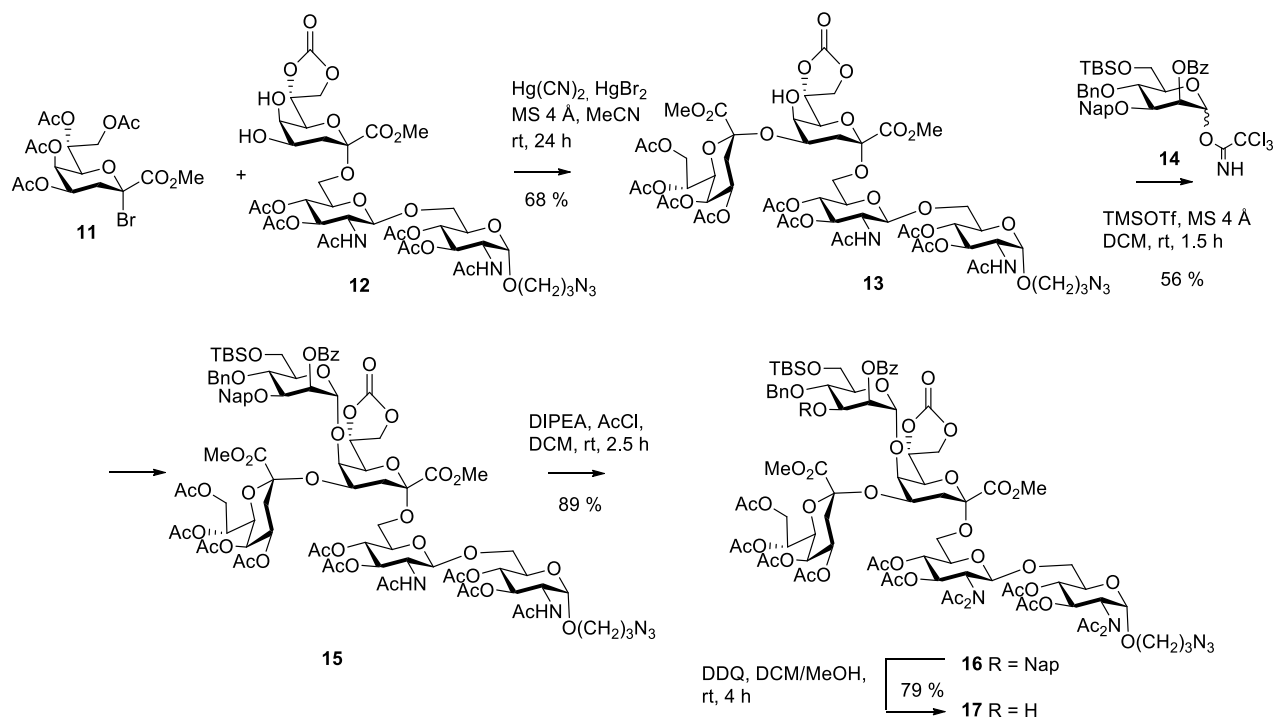
significant low-field shift of the anomeric proton of mannose B (6.49 ppm). This anomeric signal showed an HMBC correlation to a quaternary carbon signal at 162.2 ppm that was additionally correlated to a  $^1\text{H}$  NMR signal of a methyl group at 2.15 ppm. Furthermore, in an HSQC experiment, the methyl protons were found to be connected to an upfield-shifted carbon signal at 15.6 ppm. These data mirror previously reported NMR characteristics of 2-*N*-glycosyl imidates and rule out the formation of an *N*-glycosidic linkage.<sup>17</sup> The attachment site at the distal glucosamine unit could be unambiguously identified, as tracking of the spin system of the reducing GlcNAc unit could be followed from the anomeric proton to the NH signal at C-2 via COSY correlations. The imidate formation also had a significant impact on the chemical shift of C-2 of the distal glucosamine unit, which was observed at 63.8 ppm, thus in a range not usually observed for *N*-linked carbons. In contrast, the  $^{13}\text{C}$  NMR signal of C-2 of the reducing GlcNAc moiety was observed at 51.8 ppm. Thus, the  $\alpha$ -linked 3-azidopropyl spacer group most likely had sterically blocked the imidate formation at the reducing residue, and only a single imidate had been formed. This notorious side reaction of *N*-acetyl amino groups has been observed previously and is deemed responsible for the low reactivity of *N*-acetylated glycosyl acceptor derivatives in glycosylation reactions.<sup>18,19</sup>

To prevent imidate formation, conversion of *N*-acetamido groups into imides has been suggested; these can be readily reconverted into the *N*-acetamido derivatives under mild alkaline conditions.<sup>20</sup> Reaction of pentasaccharide 1 with acetyl

chloride in the presence of Hünig base proceeded smoothly and afforded the bis-*N*-acetylated derivative 5 in 89% yield. Similar to the imidate product 4, the  $^{13}\text{C}$  NMR signal of C-2 of the distal GlcNAc unit B was observed downfield shifted (61.9 ppm), whereas the signal of the reducing GlcNAc residue was detected at 56.9 ppm. The pronounced anisotropic effect of the second acetamido group on the  $\beta$ -anomeric glycoside was also reflected in a significant downfield shift of its anomeric proton, which was observed at 5.32 ppm with a coupling constant of 7.7 Hz in agreement with a *trans*-diaxial spin coupling interaction. Next, the 3-*O*-Nap group of the  $\alpha$ -mannose residue was oxidatively cleaved in a buffered system and produced the glycosyl acceptor 6 in 73% yield.

Glycosylation of 6 using 2 equiv of the mannotriacyl donor 3 and TMSO triflate as promoter was performed in dichloromethane in the presence of molecular sieves 4 Å at room temperature and afforded the  $\alpha$ -(1 $\rightarrow$ 3)-connected octasaccharide derivative 7 in a good yield of 69% (Scheme 2). The  $\alpha$ -anomeric configuration of the (1 $\rightarrow$ 3)-linked mannose unit of 7 was confirmed by the value of the heteronuclear  $J_{\text{C-1,H-1}}$  coupling constant (173.3 Hz) measured in an HMBC experiment.<sup>21</sup> Deprotection of 7 was achieved by treatment with 90% aqueous TFA, which removed the 6-*O*-*tert*-butylsilyl ether as well as both isopropylidene groups of the side-chain Kdo residue and furnished pentaol 8 in 85% yield. Full deprotection was eventually accomplished by sequential Zemplén transesterification with sodium methoxide to remove benzoyl, carbonate, and acetyl groups, hydrogenation under flow conditions, and alkaline hydrolysis of the Kdo methyl

Scheme 3. Synthesis of Alternative Pentasaccharide Acceptor 17



ester groups to afford the target octasaccharide **9** in 60% yield after final purification by size-exclusion chromatography on LH-20.  $^1\text{H}$  and  $^{13}\text{C}$  NMR data of the octasaccharide were assigned fully using COSY, TOCSY, HSQC, and HMBC experiments (see Table S1, Supporting Information) and were in generally good agreement with the published data of the *R. radiobacter* Rv3 oligosaccharide.<sup>11</sup> As expected, differences were noted for the glucosamine–phosphate backbone (see Figure 1) and carbon 8 of the lateral Kdo, which is partially substituted by an additional  $\beta$ -galactopyranosyl residue in the rhizobial LOS. The reported assignment of C-6 for the distal glucosamine unit at 70.5 ppm, however, was empirically based and needs to be corrected as the ketosidic linkage of Kdo induces only a very minor glycosylation shift of the connected carbon (63.01 ppm).<sup>22</sup> This assignment was corroborated by an HMBC correlation of a separate H-6b signal of the distal GlcNAc unit at 3.49 ppm to the anomeric signal of Kdo A. Carbons 4 and 5 of the dibranched internal Kdo unit A were shifted downfield to 71.26 and 74.40 ppm, respectively, in good agreement with literature data of comparable 4,5-*O*-disubstituted Kdo fragments.<sup>23</sup>

Initially, we had envisaged to next introduce the D3 chain after selective cleavage of the 6-*O*-TBS group in **7**, which should readily give access to glycosyl acceptor **10**. Despite many attempts using various reagents and reaction conditions, a selective desilylation could not be accomplished in a reasonable yield, due to the lability of the isopropylidene protecting groups under acidic conditions and also partial removal of the *N*-acetamido groups under basic conditions (see Table S2). As a contingency measure, introduction of the bis-acetonide using pentaol **8** was also attempted but did not lead to formation of compound **10**. Because of this impasse, we abandoned the original approach and redesigned the assembly of the pentasaccharide precursor without the isopropylidene protection of the lateral Kdo unit.

Although the well-established per-*O*-acetylated Kdo bromide methyl ester **11** exerts low  $\alpha$ -selectivity and is prone to facile elimination, leading to the corresponding 2,3-dehydro derivative, the glycosylation under Helferich conditions is nevertheless a robust approach.<sup>24</sup> Reaction of 6 equiv of donor **11** with the previously synthesized trisaccharide acceptor derivative **12**<sup>16</sup> in dry acetonitrile in the presence of a 4.5:1 mixture of  $\text{Hg}(\text{CN})_2/\text{HgBr}_2$  in dichloromethane at room temperature gave regioselectively 68% of the  $\alpha$ -linked tetrasaccharide **13** together with 11% of the corresponding  $\beta$ -anomer (Scheme 3). The anomeric mixture was resolved by column chromatography, and the anomeric configuration was assigned on the basis of the downfield shifted  $^1\text{H}$  NMR signal of H-4 (5.25 ppm for **13** and 4.85 ppm for the  $\beta$ -anomer) as well as the  $^1\text{H}$  NMR chemical shifts of the equatorial 3-deoxy protons (2.25 ppm for **13** and 2.41 ppm for the  $\beta$ -isomer).<sup>25,26</sup>

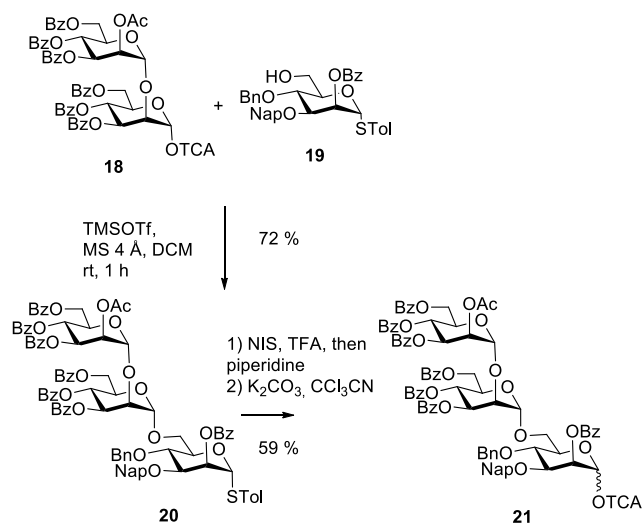
Glycosylation of the axial Kdo 5-*OH* group of **13** could next be accomplished with the previously reported mannosyl trichloroacetimidate donor **14** equipped with a 1,2-*trans*-directing 2-*O*-benzoyl group.<sup>13</sup> The glycosylation reaction—promoted by TMSO triflate in dichloromethane in the presence of molecular sieves 4 Å—proceeded to give pentasaccharide **15** in 56% yield and also allowed recovery of unreacted **13** (16%). Next, both *N*-acetamido groups were converted into the bis-imide derivative by treatment of **15** with acetyl chloride and Hünig base in dichloromethane to afford fully blocked pentasaccharide **16** in 89% yield. Oxidative removal of the 3-*O*-Nap group from **16** with DDQ furnished the stable pentasaccharide acceptor **17** in an improved yield (79%) compared to the similar transformation performed with **2**.

For the envisaged introduction of the D3 arm surrogate, the  $\alpha$ -(1 $\rightarrow$ 2)- $\alpha$ -(1 $\rightarrow$ 6)-linked mannosyl trichloroacetimidate **21** donor<sup>27</sup> was prepared. The donor was formed by a first coupling step of the known  $\alpha$ -(1 $\rightarrow$ 2)-connected trichloroacetimidate **18**<sup>28</sup> with the orthogonally protected primary alcohol



19. Thioglycoside **19** was prepared according to the literature<sup>16,29</sup> and was equipped with a 3-*O*-naphthylmethyl protecting group, which could eventually also serve for incorporation of the D2 arm. Glycosylation of **19** was promoted by catalytic TMSOTf at room temperature in dichloromethane and afforded the  $\alpha$ -(1 $\rightarrow$ 6)-linked mannotrioxide **20** in 72% yield (Scheme 4).

Scheme 4. Synthesis of Trisaccharide Donor **21**

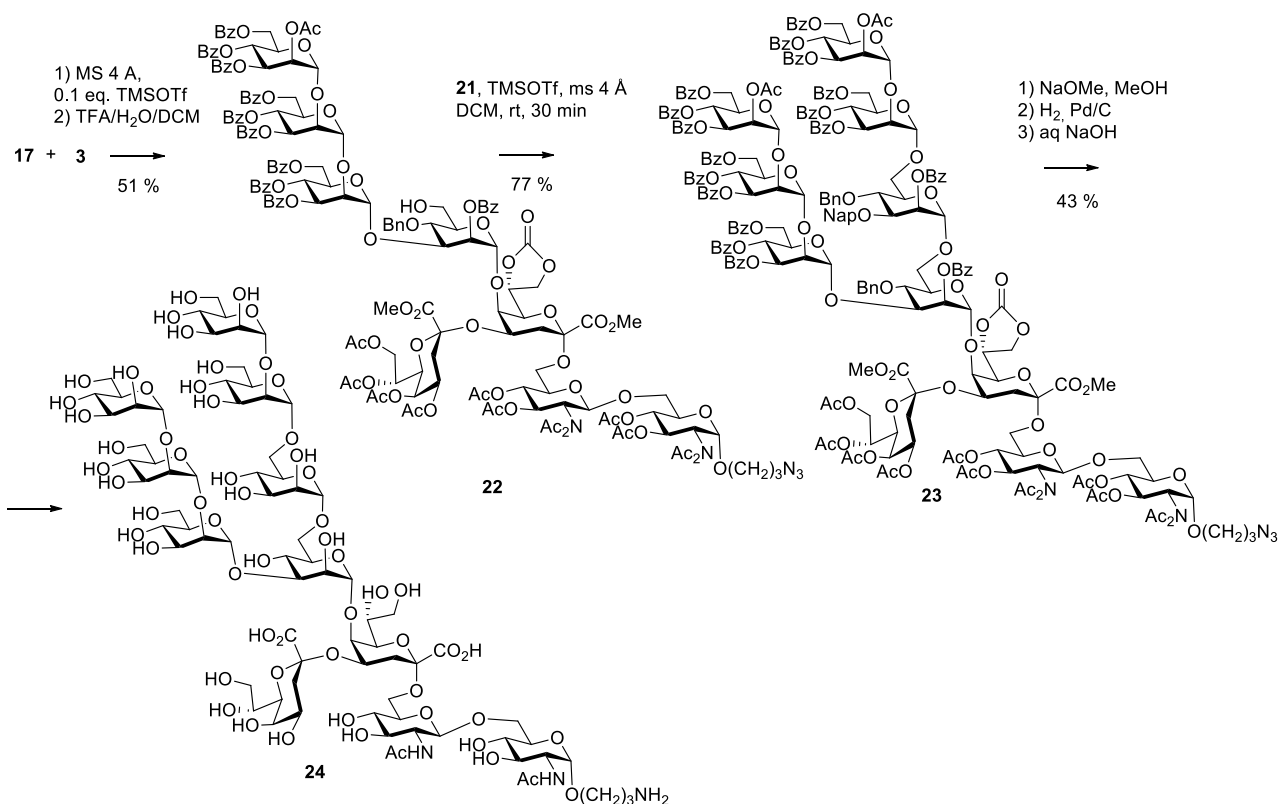


The  $\alpha$ -anomeric configuration of the internal mannose was again safely assigned on the basis of the  $J_{C-1,H-1}$  coupling constant (172 Hz). A coupling reaction of 1.8 equiv of thioglycoside **20** to pentasaccharide **17** promoted by NIS/

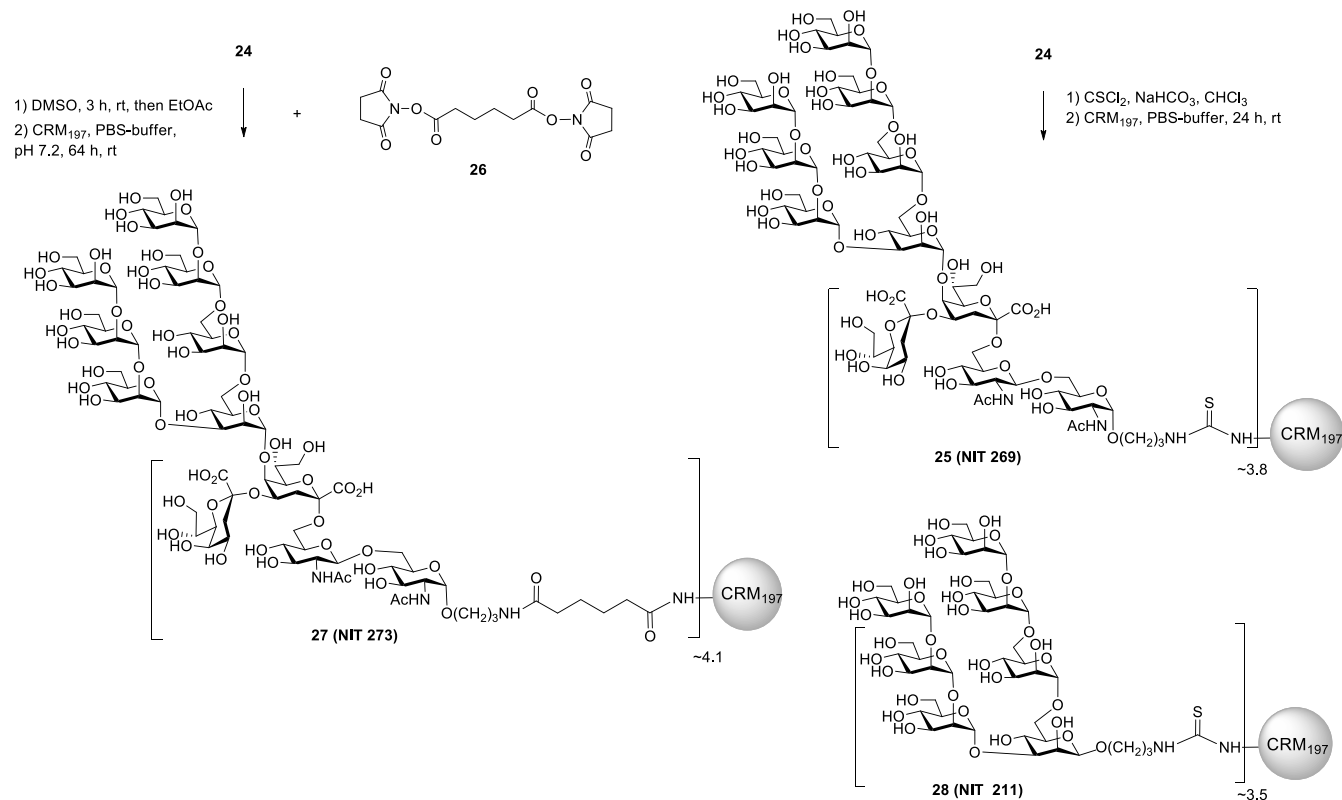
TfOH afforded a low yield (28%) of the octasaccharide product, which suggested to switch to the trichloroacetimidate donor. Hence, the anomeric thiotolyl group was cleaved by treatment with *N*-iodosuccinimide/TFA followed by conversion into the corresponding TCA donor **21** by subsequent reaction with trichloroacetonitrile/ $K_2CO_3$  in a combined yield of 59% for two steps. Proceeding toward the undecasaccharide target, pentasaccharide **17** was first coupled with the acyl-protected  $\alpha$ -(1 $\rightarrow$ 2)- $\alpha$ -(1 $\rightarrow$ 2)-linked mannotrioxyl trichloroacetimidate **3** in the presence of catalytic TMSOTf and molecular sieves 4 Å in dichloromethane, which produced the fully protected octasaccharide along with the 6-*O*-desilylated derivative **22** (Scheme 5). The mixture was directly subjected to the desilylation step by acidic hydrolysis with 90% aqueous TFA, and octasaccharide **22** was isolated in a combined yield of 51%. The 600 MHz  $^1H$  NMR spectrum in  $CDCl_3$  revealed significantly broadened signals for several mannose residues which prevented a reliable purity assessment. Spectra with improved resolution, however, could be recorded for solutions in toluene- $d_8$ . Thus, the 3-*O*-glycosylation site at the central mannose A could be confirmed by the downfield shift of H-2 at 6.02 ppm, which was in the same range as for the remaining *O*-benzoylated positions as well as the downfield-shifted  $^{13}C$  signal of carbon 3 at 76.7 ppm. This way, a potential 2 $\rightarrow$ 3 *O*-benzoyl migration could be ruled out. The final blockwise [8 + 3] glycosylation was successfully performed under similar glycosylation conditions using the octasaccharide acceptor **22** and the trisaccharide trichloroacetimidate donor **21**.

Thus, the fully protected undecasaccharide **23** was obtained in a yield of 77%, and its proton spectra were of sufficient resolution to allow for a detailed assignment. The attachment site of the branching mannose could be confirmed by the

Scheme 5. Synthesis of Undecasaccharide **24**



Scheme 6. Synthesis of Neoglycoconjugates 25 and 27 and Structure of Neoglycoconjugate 28



observed glycosylation shift of C-6 (67.1 ppm) which was similar as for the adjacent mannose unit E (for labeling of the mannosyl residues, see the [Experimental Section](#)) at 66.2 ppm.

Global deprotection was performed consecutively with intermediate control of reaction progress by NMR spectroscopy. First, acetimido, acetyl, carbonate, and benzoyl groups were removed by transesterification under Zemplén conditions that required 3 days at room temperature until completion. Next, benzyl and the NAP ether were removed by hydrogenolysis on 10% Pd carbon in a mixture of aqueous methanol/acetic acid under flow-conditions, until aromatic signals could not further be detected by NMR. Finally, saponification of the methyl ester groups in aqueous NaOH led to the fully deprotected undecasaccharide **24** isolated in 43% yield for the last three steps after HILIC purification. A full assignment of the deprotected undecasaccharide **24** suffered from severe overlap of signals, but key assignments could still be achieved, and furthermore, superposition of HSQC spectra with octasaccharide **9**, the previously synthesized core pentasaccharide<sup>16</sup> ManKdo<sub>2</sub>GlcNAc<sub>2</sub> and the 3-aminopropyl mannoheptaoside fragment<sup>13</sup> allowed for cross-checking the NMR assignments. Specifically, an HMBC correlation of the anomeric proton at 4.89 of mannose unit E to a downfield shifted methylene carbon of mannose A at 65.9 ppm was observed, confirming position 6 as the linkage site of the D3 arm. Anomeric proton and carbon signals of mannose units B-G of **24** where nearly unchanged when compared to the *manno*-heptasaccharide, but the different environment of the central mannose A linked to Kdo had a pronounced effect. Whereas <sup>1</sup>H/<sup>13</sup>C signals of the heptasaccharide ligand were observed at 4.78/100.7 ppm, signals of mannose A were downfield shifted to 5.14/101.7 ppm, probably due to the close proximity of the neighboring carboxylate of Kdo.

To assess the antigenic properties of the undecasaccharide ligand, the corresponding neoglycoconjugates were prepared using two different activation protocols for the conjugation step. Reaction conditions were chosen to incorporate a limited amount of antigen so as not to introduce glycosidic clusters that may yield unwanted neo-glycoepitopes in prospective immunization studies. Thus, spacer glycoside **24** was first reacted with thiophosgene/NaHCO<sub>3</sub> to give an intermediate isothiocyanate derivative which was then incubated with nontoxic mutant of diphtheria toxin CRM<sub>197</sub> as protein carrier<sup>30,31</sup> to give neoglycoconjugate **25**. Due to the size of the ligand, separation of unreacted ligand from the neoglycoconjugate had to be achieved by spin-filtration. Alternatively, **24** was first reacted with adipic acid bis(*N*-hydroxysuccinimide) ester **26** to afford the activated half-ester intermediate followed by coupling to the protein. MALDI-TOF analysis of the conjugates ([Figure S1](#)) revealed a comparable ligand copy number of ~3.8 for **25** and ~4.1 for **27**, respectively ([Scheme 6](#)).

As done previously,<sup>13</sup> we screened the two neoglycoconjugates by ELISA for recognition by broadly neutralizing antibodies PGT125, -126, -128, and -130, which target the high-mannose patch on HIV but interact with the oligomannose in slightly different ways.<sup>32,33</sup> A CRM<sub>197</sub> conjugate of the oligomannosidic heptasaccharide **28** was used as a comparator, as separate investigations had shown that the four aforementioned antibodies bind this conjugate, dubbed NIT211, as avidly as the earlier BSA conjugate of the same glycoside (unpublished findings). Whereas the four antibodies bound NIT211 avidly as expected, antibody binding to the undecasaccharide conjugates was unexpectedly poor ([Figure 2](#)); only PGT130 exhibited measurable binding in this assay setup.

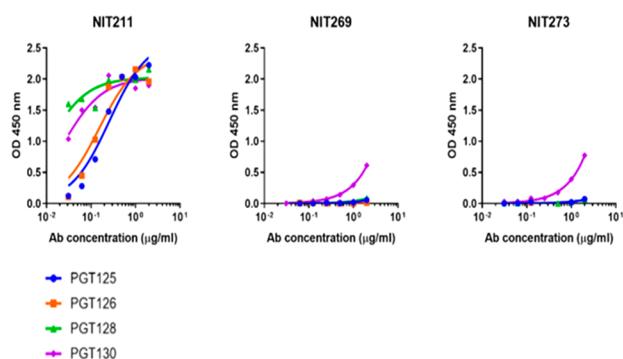


**Figure 2.** Broadly neutralizing antibodies PGT125, -126, -128, and -130 bind with relatively low avidity to CRM<sub>197</sub> conjugates of the undecasaccharide composed of an oligomannosidic heptasaccharide with a Kdo<sub>2</sub>GlcNAc<sub>2</sub> backbone. All four antibodies were tested as IgGs. NIT269 and NIT273 represent the isothiocyanate-conjugated and the adipate-conjugated glycoside, respectively. NIT211, used as a comparator, is the heptamannoside conjugated via isothiocyanate to CRM<sub>197</sub>.

To exclude influences imparted by conjugation to carrier, we performed ELISA inhibition assays with undecasaccharide **24** in comparison to the soluble oligomannosidic heptasaccharide conjugate **28**. As expected, and consistent with previous findings,<sup>13</sup> binding of all four antibodies to microtiter plates coated with conjugate NIT211 was readily inhibited (Figure S2). In contrast, no inhibition was observed with the undecasaccharide, thus corroborating the poor antibody binding observed with the corresponding CRM<sub>197</sub> conjugate.

We sought to arrive at a reasonable model for understanding these results based on structural considerations. To do so, a model of the putative interaction of PGT128 with the undecasaccharide was constructed based on the crystal structure complex of the antibody with a heptamannoside ligand (PDB ID 6B3D) and using separate crystallized fragments of the Kdo disaccharide and the lipid A backbone to guide our modeling of these portions of the undecasaccharide (Figure 3).

The modeling suggests that the side-chain Kdo (Kdo II) clashes with the antibody, in particular with HCDR2, and that, because of spatial constraints, it also may bump into the central branching mannose residue, thus likely altering the antigenic presentation of the rest of the molecule. Consistent herewith is the NMR data, showing that, with one exception, all mannose shifts for undecasaccharide are superimposable with those of the previous heptasaccharide. The noted exception is the central branching mannose (ManA), supporting the notion that the side chain Kdo is interfering with proper PGT128 binding. PGT130, which bound undecasaccharide conjugates somewhat better than PGT128 (or the other two antibodies), is believed to recognize high-mannose glycans in a mode somewhat similar to PGT128.<sup>33</sup> However, PGT130 notably lacks a 6-amino-acid insertion in HCDR2 that typifies PGT128 (and the other two antibodies), which may make it better able to accommodate the side chain Kdo and thus bind the undecasaccharide conjugates somewhat better than the other antibodies.

## CONCLUSIONS

In this study, we have undertaken a blockwise assembly of an undecasaccharide harboring a common structurally conserved fragment of bacterial lipopolysaccharides extended by two

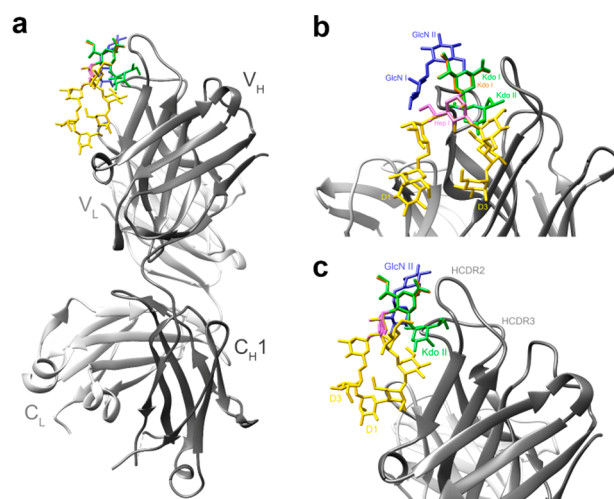


**Figure 3.** Interaction of HIV-broadly neutralizing antibody PGT128 with a model of the undecasaccharide. (a) Overview of the modeled interaction. The crystal structure complex of PGT128 with heptamannoside NIT68A<sup>13,34</sup> was used as template to create the model. The heavy and light chains of the PGT128 Fab are shown in a ribbon representation in dark gray and light gray, respectively. The modeled undecasaccharide is shown in stick representation, with the NIT68A heptamannoside in yellow, Kdo disaccharide in green, and the GlcN disaccharide in blueish purple. (b) Close-up view showing the modeled interaction of PGT128 with the undecasaccharide. The constituents of the undecasaccharide are labeled. To model the Kdo disaccharide, a crystallized Hep-Kdo<sub>2</sub> fragment<sup>35</sup> was modeled into the PGT128 binding site by superposing the heptose residue (pink) onto the central branching mannose of the NIT68A structure. To model the lipid A disaccharide, a crystallized Kdo-GlcN<sub>2</sub> fragment<sup>36</sup> was superposed onto the structure using the main-chain Kdo residue (Kdo I; orange) as a guide. (c) Left side view of panel b, highlighting the assumed proximity of the side chain Kdo (Kdo II) to the antibody.

oligomannose chains. Whereas the blockwise glycosylation steps using oligomannosyl trichloroacetimidate donors proceeded in good yields and high stereoselectivity, the synthetic route had to be modified in order to prevent imidate formation at one of the *N*-acetylglucosamine units in the glycosyl acceptor molecules. Conversion into the corresponding bis-*N*-acetylated derivatives allowed for the ensuing glycosylation steps and protecting group manipulation. In addition, isopropylidene-protecting groups at the lateral Kdo unit were not sufficiently stable to allow further chain elongation reactions and had to be replaced by acetyl groups. Deprotection allowed the synthesis and full NMR characterization of the octasaccharide fragment related to rhizobial lipooligosaccharide as well as the targeted undecasaccharide that was eventually converted into CRM<sub>197</sub> neoglycoconjugates for immunochemical studies. We used the oligomannose-specific HIV-neutralizing antibodies PGT125, -126, -128, and -130 as sentinels to gauge proper antigenic presentation of the oligomannose mimic. We observed no antibody binding (PGT125, -126, and -128) or only low antibody binding (PGT130). Modeling suggests that removing the side chain Kdo could restore antigenicity, and thus, the synthesis of such variants is now underway.



## ■ ASSOCIATED CONTENT

### Supporting Information

The Supporting Information is available free of charge on the ACS Publications website at DOI: [10.1021/jacs.9b02872](https://doi.org/10.1021/jacs.9b02872).

Experimental procedures, <sup>1</sup>H NMR and <sup>13</sup>C NMR spectra for new compounds (2, 4-9, 13, 14, 16, 17, 20-24), MALDI-TOF spectra of conjugates 25 and 27, and ELISA inhibition data of PGT125, -126, -128, and -130 with soluble ligands (PDF)

## ■ AUTHOR INFORMATION

### Corresponding Author

\*[paul.kosma@boku.ac.at](mailto:paul.kosma@boku.ac.at)

### ORCID

Paul Kosma: [0000-0001-5342-7161](https://orcid.org/0000-0001-5342-7161)

### Notes

The authors declare no competing financial interest.

## ■ ACKNOWLEDGMENTS

Financial support of this work by the Austrian Science Fund FWF (grant P 26919-N28), the Canadian Institutes of Health Research (grant IBC-150408 to R.P.), and the National Institutes of Health (grant R01 AI134299 to R.P.) is gratefully acknowledged. A Career Scholar Award by the Michael Smith Foundation for Health Research is also acknowledged (No. 5268 to R.P.). We thank Simon Krauter for the measurement of the HRMS spectra. Molecular modeling was performed with the UCSF Chimera package developed by the Resource for Biocomputing, Visualization, and Informatics at the University of California, San Francisco (supported by NIH Grant No. P41 GM103311).

## ■ REFERENCES

- (1) Fauci, A. S.; Marston, H. D. Ending AIDS - Is an HIV vaccine necessary? *N. Engl. J. Med.* **2014**, *370*, 495-498.
- (2) Bekker, L.-G.; Gray, G. E. Hope for HIV control in southern Africa: The continued quest for a vaccine. *PLoS Medicine* **2017**, *14*, No. e1002241.
- (3) Parren, P. W.; Gauduin, M.-C.; Koup, R. A.; Poignard, P.; Fiscicaro, P.; Burton, D. R.; Sattentau, Q. J. Relevance of the antibody response against human immunodeficiency virus type 1 envelope to vaccine design. *Immunol. Lett.* **1997**, *57*, 105-112.
- (4) Reitter, J. N.; Means, R. E.; Desrosiers, R. C. A role for carbohydrates in immune evasion in AIDS. *Nat. Med.* **1998**, *4*, 679-684.
- (5) Wyatt, R.; Kwong, P. D.; Desjardins, E.; Sweet, R. W.; Robinson, J.; Hendrickson, W. A.; Sodroski, J. G. The antigenic structure of the HIV gp120 envelope glycoprotein. *Nature* **1998**, *393*, 705-711.
- (6) (a) Walker, L. M.; Simek, M. D.; Priddy, F.; Gach, J. S.; Wagner, D.; Zwick, M. B.; Phogat, S. K.; Poignard, P.; Burton, D. A limited number of antibody specificities mediate broad and potent serum neutralization in selected HIV-1 infected individuals. *PLoS Pathog.* **2010**, *6*, No. e1001028. (b) Landais, E.; Huang, X.; Havenar-Daughton, C.; Murrell, B.; Price, M. A.; Wickramasinghe, L.; Ramos, A.; Bian, C. B.; Simek, M.; Allen, S.; Karita, E.; Kilembe, W.; Lakhi, S.; Inambao, M.; Kamali, A.; Sanders, E. J.; Anzala, O.; Edward, V.; Bekker, L.-G.; Tang, J.; Gilmour, J.; Kosakovsky-Pond, S. L.; Phung, P.; Wrin, T.; Crotty, S.; Godzik, A.; Poignard, P. Broadly neutralizing antibody responses in a large longitudinal sub-Saharan HIV primary infection cohort. *PLoS Pathog.* **2016**, *12*, No. e1005369. (c) Moore, P. L.; Gray, E. S.; Wibmer, C. K.; Bhiman, J. N.; Nonyane, M.; Sheward, D. J.; Hermanus, T.; Bajimaya, S.; Tumba, N. L.; Abrahams, M.-R.; Lambson, B. E.; Ranchohe, N.; Ping, L.; Ngandu, N.; Karim, Q. A.; Karim, S. S. A.; Swanstrom, R. I.; Seaman, M. S.; Williamson, C.;

Morris, L. Evolution of an HIV glycan-dependent broadly neutralizing antibody epitope through immune escape. *Nat. Med.* **2012**, *18*, 1688-1692. (d) Gray, E. S.; Madiga, M. C.; Hermanus, T.; Moore, P. L.; Wibmer, C. K.; Tumba, N. L.; Werner, L.; Mlisana, K.; Sibeko, S.; Williamson, C.; Karim, S. S. A.; Morris, L. CAPRISA 002 Study team. The neutralization breadth of HIV-1 develops incrementally over four years and is associated with CD4+ T cell decline and high viral load during acute infection. *J. Virol.* **2011**, *85*, 4828-4840. (e) Braibant, M. A.; Brunet, S.; Costagliola, D.; Rouzioux, C.; Agut, H.; Katinger, H.; Autran, B.; Barin, F. Antibodies to conserved epitopes of the HIV-1 envelope in sera from long-term non-progressors: prevalence and association with neutralizing activity. *AIDS* **2006**, *20*, 1923-1930.

(7) (a) Buchacher, A.; Predl, R.; Strutzenberger, K.; Steinfellner, W.; Trkola, A.; Purtscher, M.; Gruber, G.; Tauer, C.; Steindl, F.; Jungbauer, A.; Katinger, H. Generation of human monoclonal antibodies against HIV-1 proteins; electrofusion and Epstein-Barr virus transformation for peripheral blood lymphocyte immortalization. *AIDS Res. Hum. Retroviruses* **1994**, *10*, 359-369. (b) Trkola, A.; Purtscher, M.; Muster, T.; Ballaun, C.; Buchacher, A.; Sullivan, N.; Srinivasan, K.; Sodroski, J.; Moore, J. P.; Katinger, H. Human monoclonal antibody 2G12 defines a distinctive neutralization epitope on the gp120 glycoprotein of human immunodeficiency virus type 1. *J. Virol.* **1996**, *70*, 1100-1108.

(8) (a) Scanlan, C. N. R.; Pantophlet, R.; Wormald, M. R.; Ollmann Saphire, E.; Stanfield, R.; Wilson, I. A.; Katinger, H.; Dwek, R. A.; Rudd, P. M.; Burton, D. R. The broadly neutralizing anti-human immunodeficiency virus type 1 antibody 2G12 recognizes a cluster of  $\alpha 1 \rightarrow 2$  mannose residues on the outer face of gp120. *J. Virol.* **2002**, *76*, 7306-7321. (b) Sanders, R. W.; Venturi, M.; Schiffner, L.; Kalyanamaran, R.; Katinger, H.; Lloyd, K. O.; Kwong, P. D.; Moore, J. P. The mannose-dependent epitope for neutralizing antibody 2G12 on human immunodeficiency virus type 1 glycoprotein gp120. *J. Virol.* **2002**, *76*, 7293-7305.

(9) Doores, K. J. The HIV glycan shield as a target for broadly neutralizing antibodies. *FEBS J.* **2015**, *282*, 4679-4691.

(10) Horiya, S.; MacPherson, I. S.; Krauss, I. J. Recent strategies targeting HIV glycans in vaccine design. *Nat. Chem. Biol.* **2014**, *10*, 990-999.

(11) Clark, B. E.; Auyeung, K.; Fregolino, E.; Parrilli, M.; Lanzetta, R.; De Castro, C.; Pantophlet, R. A bacterial lipooligosaccharide that naturally mimics the epitope of the HIV-neutralizing antibody 2G12 as a template for vaccine design. *Chem. Biol.* **2012**, *19*, 254-263.

(12) Stanfield, R. L.; De Castro, C.; Marzaioli, A. M.; Wilson, I. A.; Pantophlet, R. Crystal structure of the HIV neutralizing antibody 2G12 in complex with a bacterial oligosaccharide analog of mammalian oligomannose. *Glycobiology* **2015**, *25*, 412-419.

(13) Pantophlet, R.; Trattng, N.; Murrell, S.; Lu, N.; Chau, D.; Rempel, C.; Wilson, I. A.; Kosma, P. Bacterially derived synthetic mimetics of mammalian oligomannose prime antibody responses that neutralize HIV infectivity. *Nat. Commun.* **2017**, *8*, 1601.

(14) Ang, C. W.; Noordzij, P. G.; De Klerk, M. A.; Endtz, H. P.; van Doorn, P. A.; Laman, J. D. Ganglioside mimicry of *Campylobacter jejuni* lipopolysaccharides determines antiganglioside specificity in rabbits. *Infect. Immun.* **2002**, *70*, S081-S085.

(15) Appelmelk, B. J.; Simoons-Smit, I.; Negrini, R.; Moran, A. P.; Aspinall, G. O.; Forte, J. G.; De Vries, T.; Quan, H.; Verboom, T.; Maaskant, J. J.; Ghiara, P.; Kuipers, E. J.; Bloemena, E.; Tadema, T. M.; Townsend, R. R.; Tyagarajan, K.; Crothers, J. M., Jr.; Moteiro, M. A.; Savio, A.; De Graaff, J. Potential role of molecular mimicry between *Helicobacter pylori* lipopolysaccharide and host Lewis blood group antigens in autoimmunity. *Infect. Immun.* **1996**, *64*, 2031-2040.

(16) Trattng, N.; Farcet, J.-B.; Gritsch, P.; Christler, A.; Pantophlet, R.; Kosma, P. Synthesis of a pentasaccharide fragment related to the inner core region of rhizobial and agrobacterial lipopolysaccharides. *J. Org. Chem.* **2017**, *82*, 12346-12358.

(17) Liao, L.; Auzanneau, I. The amide group in N-acetylglucosamine glycosyl acceptors affects glycosylation outcome. *J. Org. Chem.* **2005**, *70*, 6265-6273.



(18) Sekljic, H.; Wimmer, N.; Hofinger, A.; Brade, H.; Kosma, P. Synthesis of neoglycoproteins containing L-glycero- $\alpha$ -D-mannoheptopyranosyl-(1 $\rightarrow$ 4)- and - (1 $\rightarrow$ 5)-linked 3-deoxy-D-manno-oct-2-ulopyranosylonic acid (Kdo) phosphate determinants. *J. Chem. Soc., Perkin Trans. 1* **1997**, 1973–1982.

(19) Crich, D.; Dudkin, V. Why are the hydroxy groups of partially protected N-acetylglucosamine derivatives such poor glycosyl acceptors, and what can be done about it? A comparative study of the reactivity, of N-acetyl-, N-phthalimido-, and 2-azido-2-deoxy-glucosamine derivatives in glycosylation. 2-Picolinyl ethers as reactivity-enhancing replacements for benzyl ethers. *J. Am. Chem. Soc.* **2001**, *123*, 6819–6825.

(20) For examples, see: (a) Liao, L.; Auzanneau, F.-I. Glycosylation of N-acetylglucosamine: Imidate formation and unexpected conformation. *Org. Lett.* **2003**, *5*, 2607–2610. (b) Liao, L.; Auzanneau, F.-I. Synthesis of Lewis A trisaccharide analogues in which D-glucose and L-rhamnose replace D-galactose and L-fucose, respectively. *Carbohydr. Res.* **2006**, *341*, 2426–2433. (c) Ryzhov, I. M.; Korchagina, E. Y.; Popova, I. S.; Tyrtyshev, T. V.; Paramonov, A. S.; Bovin, N. V. Block synthesis of A (type 2) and B (type 2) tetrasaccharides related to the human AB blood group system. *Carbohydr. Res.* **2016**, *430*, 59–71. (d) Lafont, D.; Boullanger, P. Synthesis of N-acyl- and N-alkoxycarbonyl derivatives of 2-alkoxycarbonylamino-2-deoxy-glucose. *J. Carbohydr. Chem.* **1992**, *11*, 567–586.

(21) Bock, K.; Pedersen, C. A study of  $^{13}\text{C}$  coupling constants in hexopyranoses. *J. Chem. Soc., Perkin Trans. 2* **1974**, 293–297.

(22) Bock, K.; Thomsen, J. U.; Kosma, P.; Christian, R.; Holst, O.; Brade, H. A nuclear magnetic resonance spectroscopic investigation of Kdo-containing oligosaccharides related to the genus-specific epitope of Chlamydia lipopolysaccharides. *Carbohydr. Res.* **1992**, *229*, 213–224.

(23) For examples, see: (a) Paulsen, A.; Heitmann, A. C. Synthesis of trisaccharide units of the inner core-region of lipopolysaccharides. *Liebigs Ann. Chem.* **1989**, 1989, 655–663. (b) Pokorny, B.; Kosma, P. Synthesis of 5-O-oligoglucosyl extended  $\alpha$ -(2 $\rightarrow$ 4)-Kdo disaccharides corresponding to inner core fragments of *Moraxellaceae* lipopolysaccharides. *Carbohydr. Res.* **2016**, *422*, 5–12. (c) Yi, R.; Ogaki, A.; Fukunaga, M.; Nakajima, H.; Ichiyangi, T. Synthesis of 4,5-disubstituted 3-deoxy-D-manno-octulosonic acid (Kdo) derivatives. *Tetrahedron* **2014**, *70*, 3675–3682. (d) Kong, L.; Vijayakrishnan, B.; Kowarik, M.; Park, J.; Zakharova, A. N.; Neiwert, L.; Faridmoayer, A.; Davis, B. G. An antibacterial vaccination strategy based on a glycoconjugate containing the core lipopolysaccharide tetrasaccharide Hep2Kdo2. *Nat. Chem.* **2016**, *8*, 242–249.

(24) For recent reviews, see: (a) Pradhan, T. K.; Mong, K. K. T. Glycosylation chemistry of 3-deoxy-D-manno-oct-2-ulosonic acid (Kdo) donors. *Isr. J. Chem.* **2015**, *55*, 285–296. (b) Kosma, P. Progress in Kdo-glycoside chemistry. *Tetrahedron Lett.* **2016**, *57*, 2133–2142.

(25) Unger, F. M.; Stix, D.; Schulz, G. Structure of the 3-deoxyoctulosonic acid (Kdo) region of the lipopolysaccharide from *Salmonella minnesota* Re595. *Carbohydr. Res.* **1980**, *80*, 191–195.

(26) (a) Paulsen, H.; Stiem, M.; Unger, F. M. Synthesis of a 3-deoxy-D-manno-2-octulosonic acid (Kdo) containing tetrasaccharide and structural comparison with a degradation product from bacterial lipopolysaccharides. *Tetrahedron Lett.* **1986**, *27*, 1135–1138. (b) Kosma, P.; Strobl, M.; Allmaier, G.; Schmid, E.; Brade, H. Synthesis of pentasaccharide core structures corresponding to the genus-specific lipopolysaccharide epitope of *Chlamydia*. *Carbohydr. Res.* **1994**, *254*, 105–132.

(27) Schmidt, R. R.; Michel, J. Facile synthesis of  $\alpha$ - and  $\beta$ -O-glycosyl imidates; Preparation of glycosides and disaccharides. *Angew. Chem., Int. Ed. Engl.* **1980**, *19*, 731–732.

(28) (a) Ma, Z.; Zhang, J.; Kong, F. Synthesis of two oligosaccharides, the GPI anchor glycans from *S. cerevisiae* and *A. fumigatus*. *Carbohydr. Res.* **2004**, *339*, 29–35. (b) Zhu, Y.; Chen, L.; Kong, F. A facile regio- and stereoselective synthesis of mannose octasaccharide of the N-glycan in human CD2 and mannose

hexasaccharide antigenic factor 13b. *Carbohydr. Res.* **2002**, *337*, 207–215.

(29) Mong, K.-K. T.; Shiau, K.-S.; Lin, Y. H.; Cheng, K.-C.; Lin, C.-H. A concise synthesis of single components of partially sulfated oligomannans. *Org. Biomol. Chem.* **2015**, *13*, 11550–11560.

(30) Giannini, G.; Rappuoli, R.; Ratti, G. The amino-acid sequence of two non-toxic mutants of diphtheria toxin: CRM45 and CRM197. *Nucleic Acids Res.* **1984**, *12*, 4063–4069.

(31) Bröker, M.; Dull, P. M.; Rappuoli, R.; Costantino, P. Chemistry of a new investigational quadrivalent meningococcal conjugate vaccine that is immunogenic at all ages. *Vaccine* **2009**, *27*, 5574–5580.

(32) Sok, D.; Doores, K. J.; Briney, B.; Le, K. M.; Saye-Francisco, K. L.; Ramos, A. Promiscuous glycan site recognition by antibodies to the high-mannose patch of gp120 broadens neutralization of HIV. *Sci. Transl. Med.* **2014**, *6*, 236ra63.

(33) Doores, K. J.; Kong, L.; Krumm, S. A.; Le, K. M.; Sok, D.; Laserson, U.; Garces, F.; Poignard, P.; Wilson, I. A.; Burton, D. R. Two classes of broadly neutralizing antibodies within a single lineage directed to the high-mannose patch of HIV envelope. *J. Virol.* **2015**, *89*, 1105–1118.

(34) Pettersen, E. F.; Goddard, T. D.; Huang, C. C.; Couch, G. S.; Greenblatt, D. M.; Meng, E. C.; Ferrin, T. E. UCSF Chimera—a visualization system for exploratory research and analysis. *J. Comput. Chem.* **2004**, *25*, 1605–1612.

(35) Gomery, K.; Müller-Loennies, S.; Brooks, C. L.; Brade, L.; Kosma, P.; Di Padova, F.; Brade, L.; Evans, S. V. Antibody WN1 222–5 mimics Toll-like receptor 4 binding in the recognition of LPS. *Proc. Natl. Acad. Sci. U. S. A.* **2012**, *109*, 20877–20882.

(36) Nguyen, H. P.; Seto, N. O. L.; MacKenzie, R. C.; Brade, L.; Kosma, P.; Brade, L.; Evans, S. V. Germline antibody recognition of distinct carbohydrate epitopes. *Nat. Struct. Mol. Biol.* **2003**, *10*, 1019–1025.